Journal of
Nanoscience and Nanotechnology
Vol. 10, 3254–3259, 2010

RESEARCH ARTICLE

# Interfacial Reactions of Nano-Structured Cu-Doped Indium Oxide/Indium Tin Oxide Ohmic Contacts to *p*-GaN

Young Joon Yoon[1], S. W. Chae[2], B. K. Kim[2], Min Joo Park[3], and Joon Seop Kwak[3,*]

[1] *Fusion Technology Team, Korea Institute of Ceramic Engineering and Technology, Seoul 153-801, Korea*
[2] *Samsung Electro-Mechanics Co. Ltd., Suwon 443-743, Korea*
[3] *Department of Printed Electronics Engineering, Sunchon National University, Chonnam 540-742, Korea*

Interfacial microstructure and elemental diffusion of Cu-doped indium oxide (CIO)/indium tin oxide (ITO) ohmic contacts to *p*-type GaN for light-emitting diodes (LEDs) were investigated using cross-sectional transmission electron microscopy (XTEM), X-ray photoelectron spectroscopy (XPS), and X-ray diffraction. The CIO/ITO contacts gave specific contact resistances of $\sim 10^{-4}$ $\Omega cm^2$ and transmittance greater than 95% at a wavelength of 405 nm when annealed at 630 °C for 1 min in air. After annealing at 630 °C, multi-component oxides composed of $Ga_2O_3$-$In_2O_3$, $Ga_2O_3$-CuO, and $In_2O_3$-CuO formed at the interface between *p*-GaN and ITO. Formation of multi-component oxides reduced the barrier height between *p*-GaN and ITO due to their higher work functions than that of ITO, and caused Ga in the GaN to diffuse into the CIO/ITO layer, followed by generation of acceptor-like Ga vacancies near the GaN surface, which lowered contact resistivity of the CIO/ITO contacts to *p*-GaN after the annealing.

**Keywords:** Ohmic Contacts, Nano-Particle, GaN, Light Emitting Diode.

## 1. INTRODUCTION

GaN has been investigated and exploited for use in optoelectronic applications, such as light-emitting diodes (LEDs) and short wavelength laser diodes, as well as in high speed electronic devices.[1] In developing such devices, thermally stable, low-resistance ohmic contacts with wide processing windows are essential. Ni-, Pd-, and Pt-based *p*-type contacts, which have high work functions, are widely used as ohmic contacts to *p*-GaN with contact resistivities in the mid-$10^{-4}$ $\Omega cm^2$ range.[2,3] However, these metal-based ohmic contacts suffer from several problems, such as absorption of a significant amount of the light emitted from LEDs and the low refractive indices of the electrodes.

A number of transparent conducting oxide (TCO)-based schemes, such as indium tin oxide (ITO), zinc oxide and tin oxide, have been proposed to overcome the problems associated with metal-based ohmic contacts. Kim et al. and Margalith et al. showed that an ITO layer could be effectively used as an hole injection and current spreading layer.[4,5] Pan et al. reported that an electron-beam-evaporated nickel oxide (NiO)/ITO transparent ohmic contact produced a specific contact resistance of $\sim 10^{-3}$ $\Omega cm^2$.[6] Recently, Song et al., suggested that the transmittance and reverse-bias characteristics of TCO-based contacts are greatly improved by adding a Cu-doped indium oxide (CIO) between *p*-GaN and ITO. The lowest contact resistance was $1.5 \times 10^{-4}$ $\Omega cm^2$ and the transmittance was greater than 95% at a wavelength of 405 nm when annealed at 630 °C for 1 min in air.[7] For ohmic contacts in CIO/ITO systems, it is important to understand interfacial reactions among CIO, ITO, and GaN during the annealing process. However, there are no published reports describing changes in microstructure and chemical composition at the interface between GaN/CIO and CIO/ITO.

In the present study, microstructural and compositional characterization of CIO/ITO ohmic contacts to *p*-GaN was performed to understand interfacial reactions between CIO/ITO and *p*-GaN during annealing at 630 °C in air. The results were used to interpret changes in electrical properties during annealing. Microstructure and chemical composition at the interface between the *p*-GaN and CIO/ITO films were investigated using X-ray diffraction, X-ray photoelectron spectroscopy (XPS), angle-resolved X-ray photoelectron spectroscopy (ARXPS) and cross-sectional

*Author to whom correspondence should be addressed.


1533-4880/2010/10/3254/006 doi:10.1166/jnn.2010.2280

transmission electron microscopy (XTEM). Formation of multi-component oxides, composed of $Ga_2O_3$-$In_2O_3$, $Ga_2O_3$-CuO, and $In_2O_3$-CuO, at the interface between $p$-GaN and ITO may result in lower contact resistivity of CIO/ITO contacts to $p$-GaN.

## 2. EXPERIMENTAL DETAILS

Metalorganic chemical vapor deposition was used to grow a 2.0 $\mu$m-thick unintentionally doped GaN layer on a (0001) sapphire substrate, on which a 1.0 $\mu$m-thick $p$-GaN:Mg layer ($n_a = 5 \times 10^{17}$ cm$^{-3}$) was grown. The GaN layer was ultrasonically degreased using trichloroethylene, acetone, methanol, and deionized water (DI), each for 5 min, and then was pre-treated with buffered oxide etch (BOE) for 20 min and rinsed in DI water. After BOE treatment, circular transfer length method (CTLM) patterns were defined using a standard photolithographic technique for measuring specific contact resistance. The outer dot radius was 75 $\mu$m and the spacing between the inner and outer radii varied from 4 to 25 $\mu$m. Prior to loading in an e-beam chamber, the patterned samples were treated with buffered oxide etch (BOE) for 5 min and rinsed in DI water. The CIO (3~10 nm) and ITO (20~400 nm) films then were deposited onto $p$-type GaN by electron beam evaporation under a base pressure of $2 \times 10^{-7}$ Torr. Subsequently, some of the samples were rapid-thermal-annealed at 630 °C for 1 min in ambient air. Prior to characterizing ohmic and LED behaviors, electrical properties of the CIO/ITO films were optimized by measuring sheet resistance using a four point probe. Current–voltage ($I$–$V$) characteristics of the patterned sample and near ultraviolet InGaN/GaN LED were investigated using a parameter analyzer (HP 4155A).

Microstructural and chemical composition analyses of the sample were carried out before and after annealing using X-ray diffraction, XPS, ARXPS, and XTEM. X-ray diffraction was performed using Cu-$K\alpha$ radiation. Cross-sectional microstructures at the interface were observed using a high resolution transmission electron microscope (HRTEM) (FEI TECNAI-G2 300 kV). Chemical properties of GaN/CIO/ITO samples were characterized using XPS. The XPS measurement system (Ulvac-PHI Quantera SXM) consisted of a spherical analyzer and a monochromated Al $K\alpha$ X-ray source.

## 3. RESULTS AND DISCUSSION

The electrical and optical characteristics of CIO/ITO contacts to $p$-GaN have been briefly described in a previous study.[7] The as-deposited CIO/ITO contacts produced nonlinear $I$–$V$ characteristics. However, electrical properties of the samples were considerably improved upon annealing at temperatures in the range of 530–730 °C. CIO/ITO contacts gave specific contact resistances as low as $1.5 \times 10^{-4}$ $\Omega$cm$^2$ and transmittances greater than 95% at a wavelength of 405 nm when annealed at 630 °C for 1 min in air. Near UV LEDs fabricated with annealed CIO/ITO $p$-type contact layers showed a forward-bias voltage of 3.25 V at an injection current of 20 mA. In addition, the output power of LEDs with CIO/ITO contacts was enhanced by 78% at 20 mA, as compared with those of LEDs with conventional Ni/Au contacts.

To understand the mechanism by which good ohmic contacts to $p$-GaN form using a completely oxide-based contact scheme, i.e., the CIO/ITO scheme, microstructural and compositional analyses of the samples were carried out before and after annealing. First, X-ray diffraction with glancing angle incidence was used to investigate grain size and orientation of CIO/ITO films before and after annealing. Figure 1(a) and (b) show X-ray diffraction patterns of as-deposited CIO (10 nm)/ITO (200 nm) on $p$-type GaN and of CIO/ITO annealed at 630 °C, respectively. X-ray diffraction patterns of the as-deposited films, as shown in Figure 1(a), exhibited a broad peak, suggesting formation of amorphous-like structures. After annealing at 630 °C, however, the broad peak disappeared and sharp peaks corresponding to ITO were observed, indicating the formation of polycrystalline ITO films.

Interfacial microstructures of the CIO/ITO contacts to $p$-GaN were analyzed using XTEM. The XTEM micrograph for the as-deposited samples, as shown in Figure 2(a), shows small grains, having a crystal structure of $In_2O_3$, at the interface. In addition, irregular islands having an amorphous structure were observed on the surface of GaN, as shown in Figure 2(b). After annealing at 630 °C, however, the amorphous islands at the interface disappeared and nano-sized grains, which showed crystallinity different from that of $In_2O_3$, were observed at the

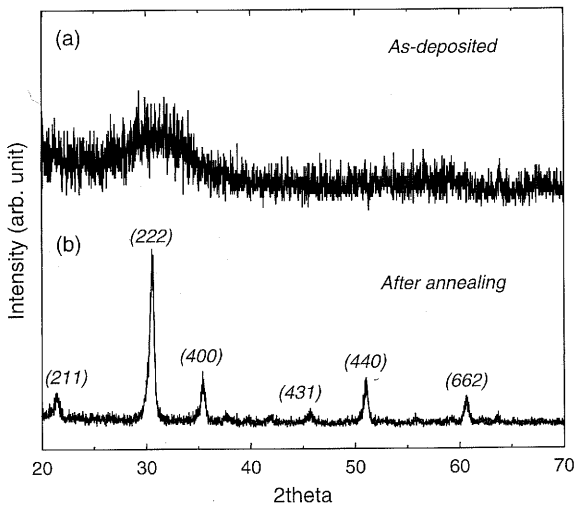


**Fig. 1.** Grazing angle X-ray diffraction patterns of CIO (10 nm)/ITO (200 nm) on $p$-GaN (a) The XRD pattern of as-deposited sample, (b) The XRD pattern of sample annealed at 630 °C for 1 min.

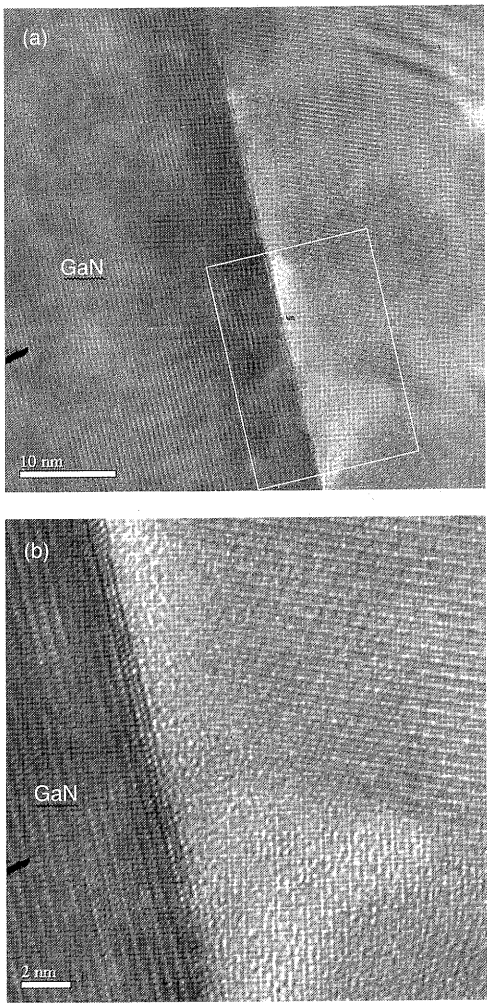


**Fig. 2.** High-resolution XTEM image of as-deposited CIO (10 nm)/ITO (200 nm) on *p*-type GaN, (a) The XTEM image at the interface, (b) The magnified image of the area indicated by the box in (a).

interface between the GaN and ITO, as shown in Figure 3. The chemical and structural properties of the nano-size grains could not be fully characterized using XTEM due to complicated diffraction patterns caused by small grain size and to overlap with the $In_2O_3$ matrix. However, new compounds appeared to form at the interface between ITO and GaN after annealing at 630 °C. Characterization of these compounds, as well as of the amorphous islands observed in the as-deposited samples, is the key to clarifying the mechanism by which CIO/ITO ohmic contacts to *p*-GaN form.

To characterize the interfacial reactions between CIO/ITO contacts to *p*-GaN, distributions of the chemical elements of the as-deposited and annealed GaN/CIO/ITO samples were analyzed using XPS with high resolution Ar ion sputter-depth profiling (3 kV ion energy) and Zalar rotation. Figure 4 shows the XPS depth profiles for the as-deposited sample; only the spectra for sputter times between 10 and 30 min are shown to clearly illustrate the interfacial reactions between CIO/ITO and

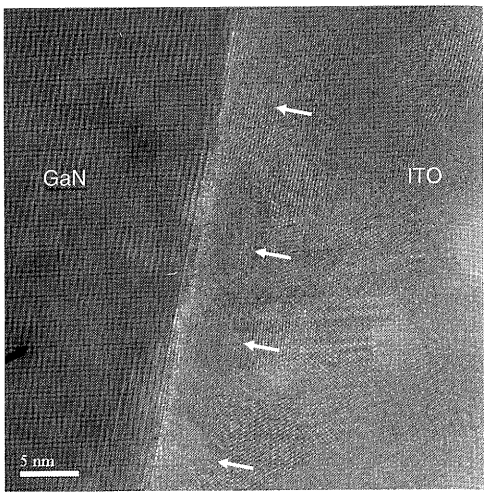


**Fig. 3.** High-resolution XTEM image of annealed CIO (10 nm)/ITO (200 nm) on *p*-type GaN. The arrows indicate the nano-sized grains at the interface.

GaN. The resolved spectrum of In $3d_{5/2}$ near the interface between CIO/ITO and GaN, as shown in Figure 4(a), exhibited a main component at 444.9 eV, corresponding to $In_2O_3$. However, as the sputtering time was increased up to 22 min, a small peak at 443.8 eV appeared, which was attributed to the metallic In state that does not bind oxygen. The resolved spectrum of the Cu $2p_{3/2}$ peak, as shown in Figure 4(d), also indicates that, during deposition of the CIO layer, most Cu existed in the metallic state (932.7 eV). It is worth while to note that the *I–V* curve was not linear at the as-deposited state of CIO/ITO contacts to *p*-GaN, which may be attributed to the existence of metallic In and Cu after the deposition.[7] An oxidized Ga state assigned to $Ga_2O_3$ at 1117.8 eV was detected in the as-deposited sample after sputtering times of 22 and 23 min for, as shown in Figure 4(c). To compare the results of the XPS and XTEM analyses, shown in Figures 2(b) and 4(c), respectively, the amorphous irregular islands observed at the interface between the GaN and ITO for the as-deposited sample were the native oxide mainly composed of $Ga_2O_3$. These results imply that, in spite of the chemical treatment using BOE for 5 min prior to deposition of CIO/ITO films, the native oxide was not fully removed.

A significant interfacial reaction occurred after annealing at 630 °C. The distributions of chemical elements measured by XPS depth profiling are shown in Figure 5. Since the sputtering of the 200 nm-thick ITO film in the annealed sample took more times that that in the as-deposited sample, only the spectra for sputter times ranging from 40 to 80 min are shown to illustrate the interfacial reactions between CIO/ITO and GaN more clearly. Spectra of annealed samples were quite different from those of as-deposited samples. The resolved spectrum of In 3d, as shown in Figure 5(a), exhibited a component at 444.9 eV, corresponding to $In_2O_3$, which implies that metallic In

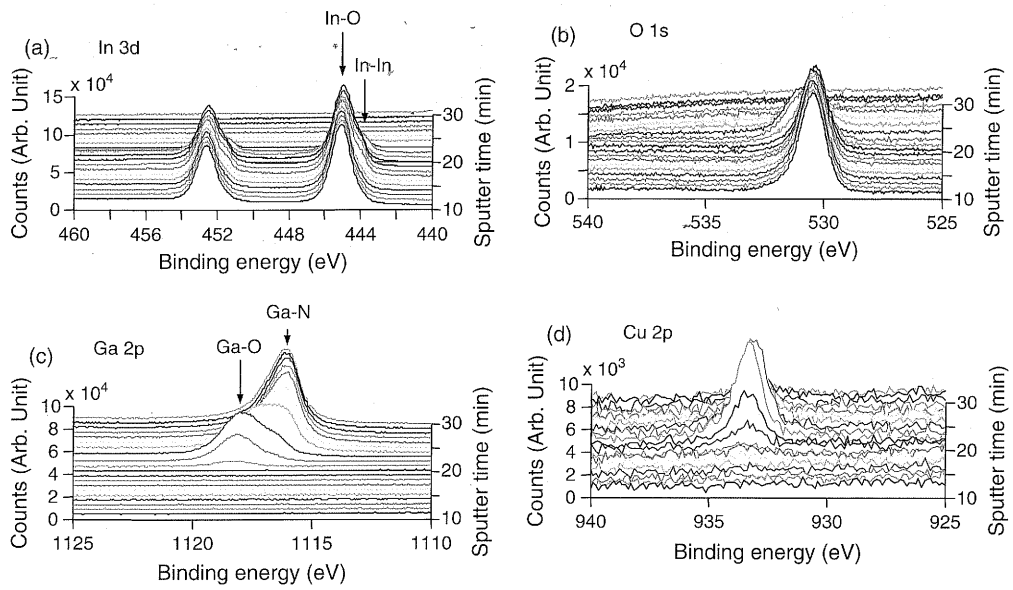


**Fig. 4.** Evolution of the XPS fine spectra of In 3d (a), O 1s (b), Ga 2p (c), and Cu 2p (d) near the interface between ITO and GaN in the as-deposited sample as sputtering time increases.

at the as-deposited state (shown in Fig. 4(a)) fully converted to In-oxide after the annealing. However, as shown in Figure 5(d), it was impossible to assign the state of Cu due to its low concentration, which may be caused by significant diffusion of Cu into ITO and GaN. A peculiar charging shift toward lower binding energy in whole elements, which was seen near a sputter time of 60 min (Fig. 5), was observed near the interface, despite application of a neutralization system with low Ar ion energy (<a few tens of eV) and of an electron flood. Presently, the reason for this charging shift remains unclear; however, it may have originated from formation of a new compound, which had a conductivity different from those of ITO and GaN.

To clearly understand the interfacial reaction between CIO/ITO and *p*-GaN after annealing at 630 °C, high-resolution ARXPS was applied to the annealed sample, as shown in Figure 6. The non-destructive depth profiling using ARXPS eliminates artifacts that result from Ar ion sputtering, such as preferential sputtering, ion beam mixing and elemental damage, which can result in precise chemical states across the interface.[8] To perform ARXPS, most of the ITO layer in the CIO/ITO contact scheme was removed using Ar ion sputtering until region A, shown in the Figure 6(a), was exposed, then the take-off angle was changed from 10 to 90 degrees. After analyzing region A, additional Ar ion sputtering was performed to expose regions B and C, as shown in Figure 6(a). Again,

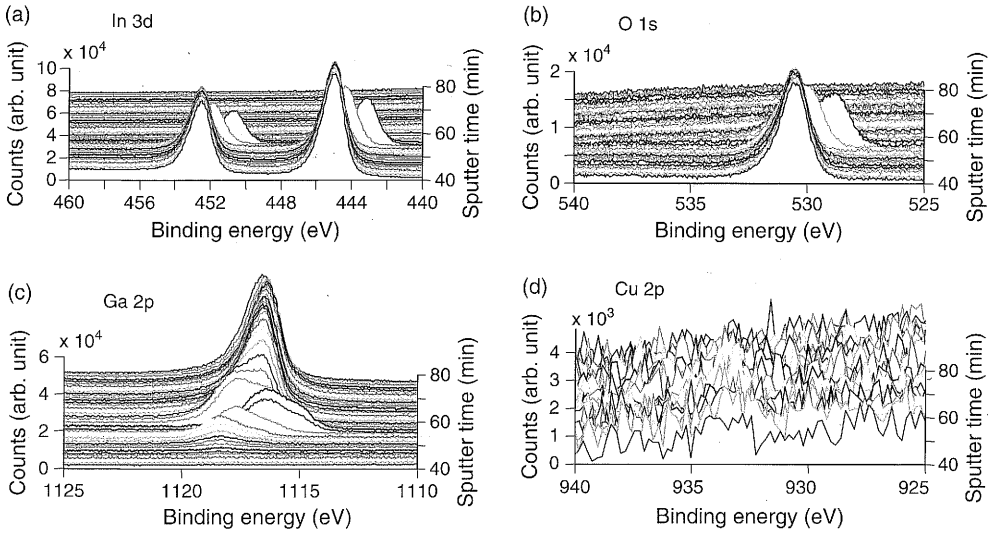


**Fig. 5.** Evolution of the XPS fine spectra of In 3d (a), O 1s (b), Ga 2p (c), and Cu 2p (d) near the interface between ITO and GaN in the sample annealed at 630 °C for 1 min as sputtering time increases.

the take-off angle was changed from 10 to 90 degrees to obtain non-destructive depth profiling spectra of elements in regions B and C, respectively. Figures 6(b)–(d) show ARXPS spectra of In 3d, O 1s, Ga 2p, and Cu 2p, while varying the take-off angle from 10 to 90°, measured in regions A, B, and C of Figure 6(a), respectively. The resolved spectrum of In 3d exhibited only a component at 444.9 eV, corresponding to $In_2O_3$. It is worthy of notice that Cu, which was not detectable in sputter-depth profiling due to its low concentration (shown in Fig. 5(d)), was detected using high-resolution ARXPS. The chemical state of Cu was assigned to CuO, which indicates that metallic Cu at the as-deposited state (shown in Fig. 4(d)) fully converted to CuO after annealing at 630 °C.

Non-destructive depth profiling of the atomic element concentration in each region was calculated from the intensity of spectrum. Figures 7(a)–(c) show relative concentrations of In, Ga, O, and Cu, while varying the take-off angle in regions A, B, and C, respectively. There was a significant interfacial reaction among CIO, the $Ga_2O_3$ native oxide and *p*-GaN after annealing at 630 °C. As shown in Figure 7(a), the main component in region A of Figure 6(a) was $In_2O_3$ with small amounts of $Ga_2O_3$ and CuO. In region B of Figure 6(a), the main component was $Ga_2O_3$ combined with $In_2O_3$ and CuO, as also shown in Figure 7(b). In region C, which was close to *p*-GaN, the In signal was not detected, although, $Ga_2O_3$ and CuO peaks were observed at low take-off angles. The thickness of the $Ga_2O_3$ combined with $In_2O_3$ and CuO should not exceed 10 nm, considering the inelastic mean free path of photoelectrons from the Ga 2p shell. The XTEM results shown in Figure 3 were consistent with the estimated thickness. The ARXPS results suggest that the new compounds having nano-sized grain structures, which were detected using XTEM at the interface (Fig. 3), could be multi-component oxides composed of $Ga_2O_3$-$In_2O_3$ and $Ga_2O_3$-CuO. The region between the new compounds having nano-sized grain structures may be composed of $In_2O_3$ and CuO.

Based on microstructural and chemical composition analyses of CIO/ITO contacts to *p*-GaN using X-ray diffraction, XTEM, XPS, and ARXPS, the anneal-induced improvement in the electrical properties of CIO/ITO contacts may be explained as follows. ARXPS results for the 630 °C-annealed samples (Figs. 6 and 7) demonstrated that Ga in the GaN diffused outward into the CIO/ITO layer and participated in the formation of multi-component oxides composed of $Ga_2O_3$-$In_2O_3$ and $Ga_2O_3$-CuO. The formation of Ga-based oxides produces Ga vacancies near the GaN surface, which may cause generation of acceptor-like Ga vacancies. This led to a reduction in Schottky barrier height and, therefore, to a reduction in contact resistivity.[9, 10] Second, the improved electrical properties could be related to the formation of $Ga_2O_3$-$In_2O_3$ and $In_2O_3$-CuO. Minami et al. reported that $GaInO_3$

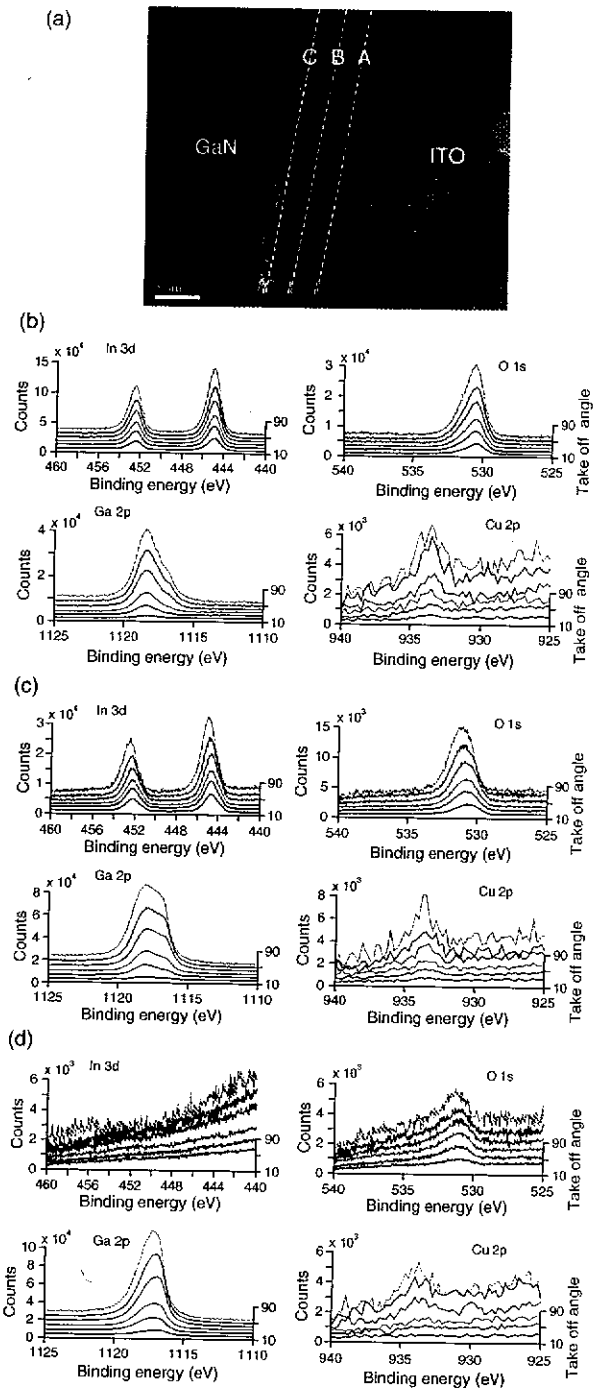


**Fig. 6.** ARXPS fine spectra of In 3d, O 1s, Ga 2p, and Cu 2p while varying the take-off angle from 10 to 90°. The spectra shown in Figures 6(b)–(d) were obtained near regions A, B, and, C (shown in the XTEM image of Fig. 6(a)), respectively.

has a higher work-function (~5.4 eV) than those of ITO (~4.7 eV) and $In_2O_3$ (~4.8 eV).[11] In addition, Kawazoe et al. suggested that, based on chemical bond analysis, Cu-In-oxides can be *p*-type transparent conducting oxides.[12] The formation of high work function compounds, such as $Ga_2O_3$-$In_2O_3$ and $In_2O_3$-CuO, which reduces the Schottky barrier height and, hence, decreases contact resistivity

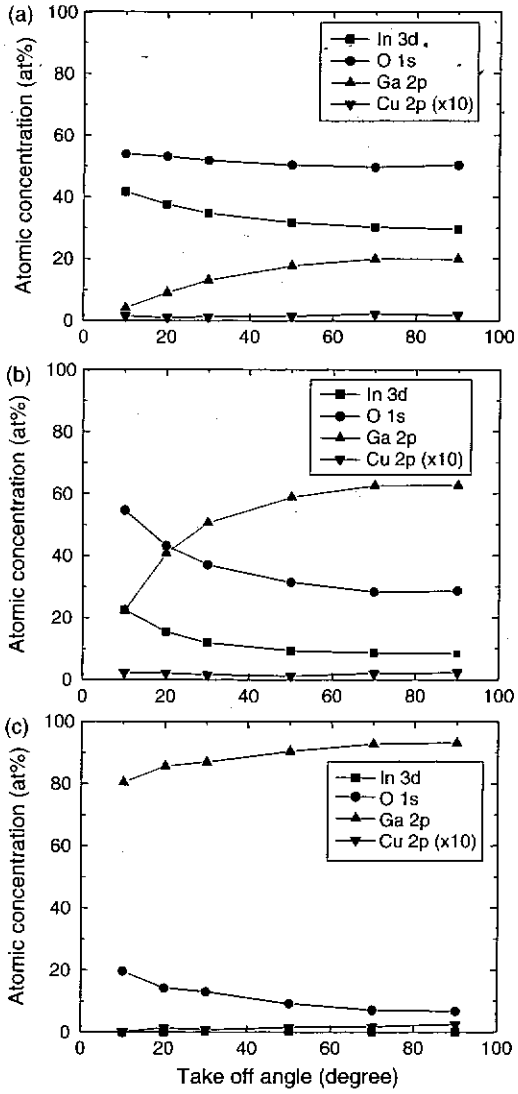


**Fig. 7.** Relative atomic concentrations of In 3d, O 1s, Ga 2p, Cu 2p and Sn 3d while varying the take-off angle from 10 to 90°. Figures 7(a)–(c) were obtained from Figures 6(b)–(d), respectively.

of the CIO/ITO contacts to *p*-GaN, may lead to an increase in work function of the electrodes compared with as-deposited samples.

## 4. CONCLUSION

Interfacial microstructures and elemental diffusion of CIO/ITO ohmic contact to *p*-type GaN were investigated using X-ray diffraction, XTEM, XPS, and ARXPS. The CIO/ITO contacts gave specific contact resistances of $\sim 10^{-4}$ $\Omega cm^2$ and transmittances greater than 95% at a wavelength of 405 nm when annealed at 630 °C for 1 min in air. After annealing at 630 °C, new multi-component oxides composed of $Ga_2O_3$-$In_2O_3$ and $Ga_2O_3$-CuO were produced at the interface between *p*-GaN and ITO, and $In_2O_3$-CuO was also formed between the new compounds. Formation of new oxides such as $Ga_2O_3$-$In_2O_3$ and $In_2O_3$-CuO, having higher works function than that of ITO, reduced the barrier height between *p*-GaN and ITO, hence decreasing contact resistivity of the CIO/ITO contacts to *p*-GaN. In addition, the formation of Ga-based oxides ($Ga_2O_3$-$In_2O_3$ and $Ga_2O_3$-CuO), caused Ga in the GaN to diffuse outward into the CIO/ITO layer, followed by generation of acceptor-like Ga vacancies near the GaN surface. This increase in carrier concentration near the GaN surface, reduced Schottky barrier height and, hence, lowered contact resistivity.

**Acknowledgment:** This work was supported by the Korea Science and Engineering Foundation (KOSEF) grant funded by the Korea government (MEST) (No. 2009-0080313). This research was also supported by the WCU program at Sunchon National University and by the Ministry of Knowledge Economy through the project of Regional Innovation Center (RIC).

## References and Notes

1. S. Nakamura and G. Fasol, The Blue Laser Diode, 1st edn., Springer-Verlag, Heidelberg (**1997**), p. 8.
2. J. Ho, C. Jong, C. C. Chiu, C. Huang, C. Chen, and K. Shih, *Appl. Phys. Lett.* 74, 1275 (**1999**).
3. J. S. Kwak, J. Cho, S. Chae, K. K. Choi, Y. J. Sung, S. N. Lee, O. H. Nam, and Y. Park, *Phys. Stat. Sol. (A)* 194, 587 (**2002**).
4. D. W. Kim, Y. J. Sung, J. W. Park, and G. Y. Yeom, *Thin Solid Films* 398–399, 87 (**2001**).
5. T. Margalith, O. Buchinsky, D. A. Cohen, A. C. Abare, M. Hansen, S. P. DenBaars, and L. A. Coldren, *Appl. Phys. Lett.* 74, 3930 (**1999**).
6. S.-M. Pan, R.-C. Tu, Y.-M. Fan, R.-C. Yeh, and J.-T. Hsu, *IEEE Photonics Technol. Lett.* 15, 646 (**2003**).
7. J.-O. Song, J. S. Kwak, Y. Park, and T.-Y. Seong, *Appl. Phys. Lett.* 86, 213505 (**2005**).
8. P. J. Crumpson, *J. Electron. Spectrosc. Relat. Phenom.* 73, 25 (**1995**).
9. J.-O. Song, D.-S. Leem, and T.-Y. Seong, *Appl. Phys. Lett.* 83, 3513 (**2003**).
10. J. S. Kwak, J.-O. Song, T.-Y. Seong, B. I. Kim, J. Cho, C. Sone, and Y. Park, *J. Nanosci. Nanotechnol.* 6, 3547 (**2006**).
11. T. Minani, *J. Vac. Sci. Technol. A* 17, 1765 (**1999**).
12. H. Kawazoe, M. Yasukawa, H. Hyodo, M. Kurita, H. Yanagi, and H. Hosono, *Nature* 389, 939 (**1997**).

Received: 1 January 2009. Accepted: 1 July 2009.